



Synthesis and Characterization of Pure and Sn-Doped CeO₂ Nanoparticles

K. SURESH KUMAR* and N. VICTOR JAYA

Department of Physics, College of Engineering, Anna University, Chennai-600 025, India

*Corresponding author: E-mail: ksuresh_1979@yahoo.co.in

(Received: 4 July 2012;

Accepted: 29 April 2013)

AJC-13409

Nanoporous pure and Sn-doped CeO₂ were synthesized *via* chemical precipitation technique. The structural and optical properties of the prepared ceria nanoparticles were characterized using analytical experimental techniques. X-ray diffraction pattern of the samples shows the formation of single phase cubic structured CeO₂ nanoparticles without any secondary impurities. This result was supported by Fourier transform infrared spectroscopy analysis. The porous surface morphology of the nanoparticles was visibly observed from scanning electron microscopy. Optical activity of the samples were measured through UV-visible diffuse reflectance spectroscopy spectrophotometer which shows strong UV absorption band about 300 nm for the pure and doped samples. The extrapolated optical band gap energy values are 4.85 eV and 5.04 eV for the pure and 6 mol % Sn doped CeO₂ respectively.

Key Words: Cerium oxide, Nanoparticles, Chemical precipitation, Sn-Doped ceria, Energy band gap.

INTRODUCTION

Cerium oxide or Ceria (CeO₂) has been widely investigated owing to its broad spectrum of scope to be examined such as catalyst, polishing media and ceramic material for high temperature devices¹. It acts as an electrolyte substance in solid oxide fuel cells as well². Ceria is a large bandgap 3.55 eV semiconductor material mainly used for catalytic purposes³.

In the recent past, nano ceria has made an impact towards the biomedical engineering to inhibit cellular ageing⁴. Bamwenda *et al.*⁵ have reported that cerium oxide is a potential photo catalyst that can be used to decompose water in order to produce oxygen. Corma *et al.*⁶ voiced the potential use of zirconium and lanthanum doped CeO₂ nanoparticles in solar cell devices.

The potential application and unique characteristic behaviour of CeO₂ has given due interest to study their properties in depth. Understanding the electronic and structural modification of CeO₂ is one of the most important factors for their commercial application. Electrical resistivity and thermal stability of the metal oxides strongly depends on the structural change of the nanoparticles due to compression or high temperature.

One among the various metals, tin is most abundant and low cost material. It possesses many unique chemical, electronic and optical properties. It is advantageous in several applications, such as solar cells, catalysis and gas-sensing applications⁷. In this paper, we report that the ultra fine Sn-doped CeO₂

nanoparticles were prepared by a simple precipitation method. The prepared samples were characterized to investigate their structural and morphological properties at the nanoscale as a function of dopant concentration.

EXPERIMENTAL

Synthesis of pure and Sn-doped CeO₂ nanoparticles: Analytical grade cerium nitrate hexahydrate [Ce(NO₃)₃·6H₂O] and tin chloride (SnCl₂·2H₂O) were used as received without any further purification. The cerium oxide nanoparticles were prepared by chemical precipitation method which comprises the steps of mixing, stirring and calcination. Briefly, 0.1 M aqueous solution of Ce(NO₃)₃·6H₂O was prepared under constant stirring. After 10 min, the ammonia solution was added drop wise to the above solution until the pH reaches to 10. The stirring was continued for another 2 h for the complete precipitation. Finally, the precipitate was washed thoroughly with ultra pure double distilled water repeatedly for several times under sonication. The end product was dried at 100 °C for 24 h and then the powder was calcined at 600 °C for 5 h to promote the crystallization. For the Sn-doped CeO₂ nanoparticles the same synthesis procedure was followed with the addition of three different compositions tin chloride (4, 6 and 8 mol %) to aqueous Ce(NO₃)₃·6H₂O solution.

Characterization techniques: The XRD pattern for the materials was analyzed on a Rigaku 2550D/Max VB/PC advance X-ray diffractometer (XRD) with CuK_α radiation (wavelength of 1.54056 Å). The SEM studies were carried out using

Hitachi S-3400 apparatus to study the surface morphology of the ceria nanoparticles. Fourier transform infrared spectroscopy of the sample was analyzed using Perkin-Elmer FTIR spectrometer over the wavenumber between 4000-400 cm^{-1} . UV-visible diffuse reflectance spectroscopy of the prepared samples were taken in UV-2450 Shimadzu UV-visible spectrophotometer.

RESULTS AND DISCUSSION

XRD analysis: Fig. 1 shows the XRD patterns of the pure and Sn-doped cerium oxide nanoparticle with larger broadening of peaks, which in turn leads to a small particle size. All the peaks indexed to a pure cubic fluorite structure (JCPDS 34-394) of CeO_2 with lattice constant 'a' = 5.411 Å. The intensive diffraction peak is located at $2\theta = 28.66, 33.07, 47.48$ and 56.34° , corresponding to (111), (200), (220) and (311) lattice planes respectively. They are well matched with the peaks of face centered cubic crystal structure⁸. Due to the Sn^{2+} doping the crystallite of the CeO_2 considerably decreases when compared to pure CeO_2 . This can be seen from the well defined peak broadening in the XRD pattern of the doped samples as in Fig. 1(b-d). In addition to the above, all the peaks are shifted towards lower angle, which indicates the decrease in volume of the crystal. The average crystallite size and lattice parameter of the pure and Sn doped CeO_2 nanoparticles are given in Table-1. The mean diameter of the nanoparticles are calculated using Scherrer's equation⁹.

$$D = 0.9\lambda/\beta\cos\theta$$

where, β is the full width half maximum value of maximum intensity peak, θ - diffraction angle and λ - Wavelength of the X-rays (1.5408 Å).

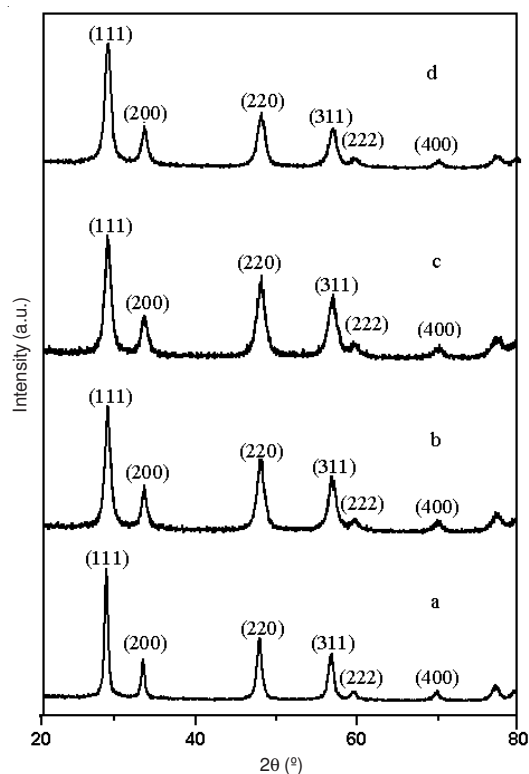


Fig. 1. XRD patterns of pure (a) and 4, 6 and 8 mol % (b-d) of Sn-doped CeO_2 nanoparticles

TABLE-1			
Composition/ 600 °C	Lattice parameter 'a' (Å)	Unit cell volume 'a' ³ (Å ³)	Mean crystallite size (nm)
Pure CeO_2	5.365	154.42	25.56
4 mol % Sn- CeO_2	5.349	153.04	25.48
6 mol % Sn- CeO_2	5.346	152.78	21.20
8 mol % Sn- CeO_2	5.269	148.32	17.14

FT-IR analysis: FT-IR spectra of pure and Sn doped CeO_2 samples are represented in Fig. 2. The spectra clearly shows three intense bands positioned at 3420, 1614 cm^{-1} and below 700 cm^{-1} . The broad absorption bands at 3420 and 1614 cm^{-1} are associated to the symmetric stretching (ν OH) and bending modes of (δ OH) internally bonded water molecules respectively. The more intense band is observed at 2380 cm^{-1} for 6 % Sn doped CeO_2 when compared to pure CeO_2 . This confirms that the additional CO_2 was absorbed at CeO_2 surface with the addition of Sn. Furthermore the O-C-O stretching band also observed in the 1600-1300 cm^{-1} region. The bending mode of Ce-O-C (δ) is observed well below 700 cm^{-1} and affirms the formation CeO_2 without impurities¹⁰. The peak positioned at 450 to 550 cm^{-1} is attributed to the O-Ce-O stretching mode of vibration^{11,12}. This FTIR study fairly agrees with the XRD results.

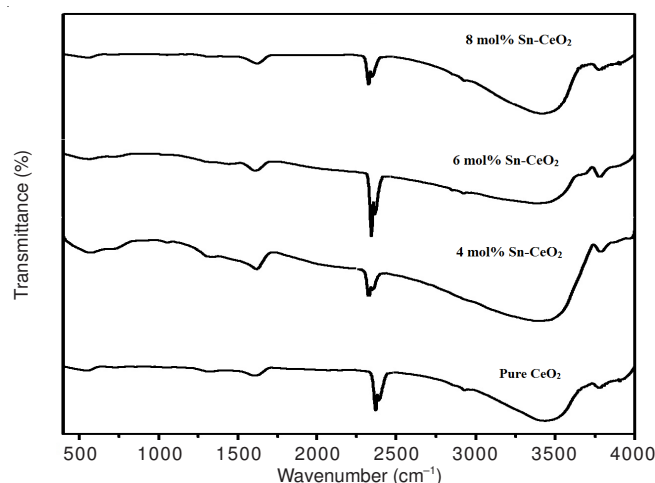


Fig. 2. FT-IR spectra of pure and Sn-doped CeO_2 nanoparticles

Morphological studies: The SEM images of pure and 6 mol % Sn-doped CeO_2 nanoparticles are shown in the Fig. 3 (a) and (b). It is clearly visible that the particles are highly aggregated and exhibit porous nature¹³. Both the samples show identical surface morphology. In the case of 6 mol % Sn^{2+} doping more agglomeration was observed. Ultrafine nanoparticles tend to agglomerate. This confirms the reduction in crystallite size significantly by adding Sn ions to CeO_2 host. The quantitative elemental analysis is performed using EDS. The observed EDS spectrum of pure and 6 mol % Sn^{2+} doped CeO_2 is shown in Fig. 4(a) and (b). From the spectrum, that the cerium and tin absorption was strongly observed, which confirms the stoichiometric concentration of the elements.

UV-visible diffuse reflectance spectrum analysis: UV-visible absorption spectra of pure and Sn-doped CeO_2 was shown in Fig. 5(a). It indicates the strong absorption at 300

nm and 310 nm for pure and doped CeO₂ nanoparticles. The absorbance peak slightly shifted towards low energy side due to Sn incorporation into Ce. The observed UV region absorption band confirm the direct electron transition between Ce⁴⁺ and O²⁻ in CeO₂. Direct energy optical band gap is determined using the Kubelka-Munk function¹⁴.

$$F(R) = (1-R)^2/2R$$

Linearly extrapolated absorption curves at real axis gives the band gap energy E_g as shown in Fig. 5(b). The obtained E_g values of the pure and 6 mol % Sn doped CeO₂ are 4.85 eV and 5.04 eV respectively. This E_g values are quite high when

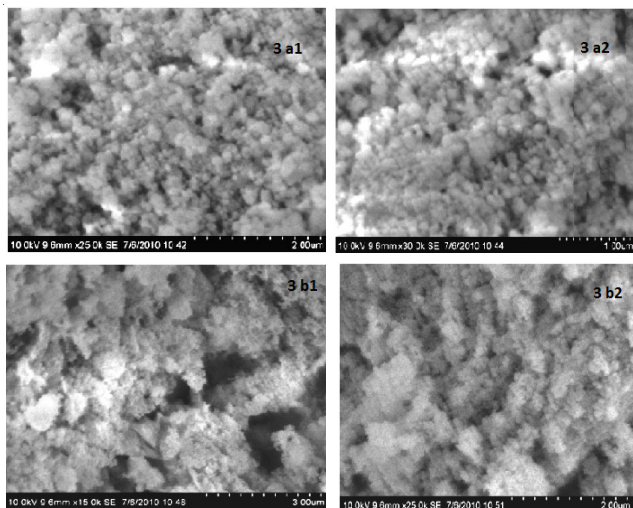


Fig. 3. a) SEM images pure CeO₂ with different magnifications; b) SEM images of 6 mol % of Sn-doped CeO₂ nanoparticles with different magnifications

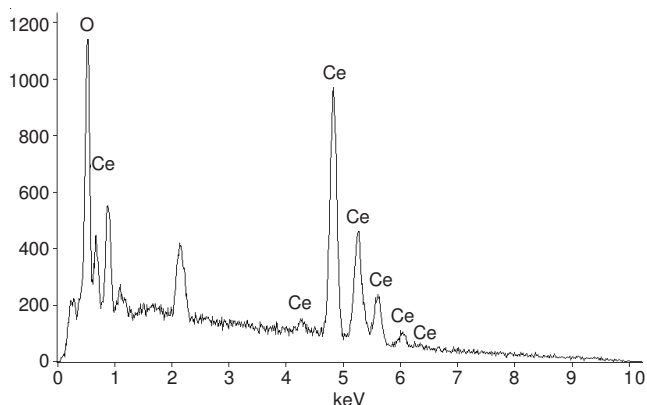


Fig. 4. (a) EDS spectrum of pure CeO₂ nanoparticles

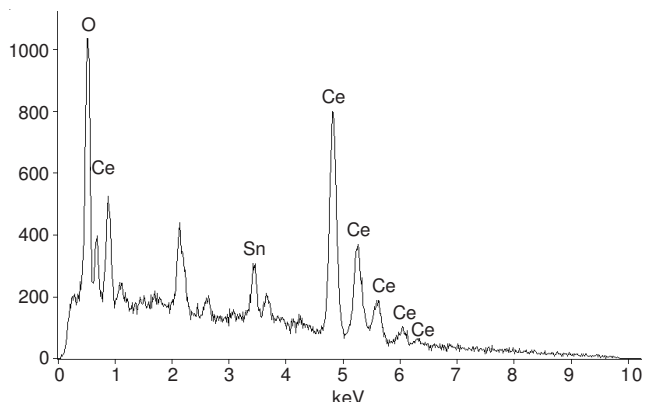


Fig. 4. (b) EDS spectrum of 6 mol % of Sn-doped CeO₂ nanoparticles

compared to earlier reports^{15,16}. In present case, the Sn doped sample shows large E_g than the pure CeO₂. It indicates the size dependent quantum confinement of the nanoparticles¹⁷. For the doped cerium oxide shows the shift in energy band concludes that the large number of electron-hole confinement. This may be due to the presence of Sn²⁺ in Ce⁴⁺ site which provides additional holes for trapping process.

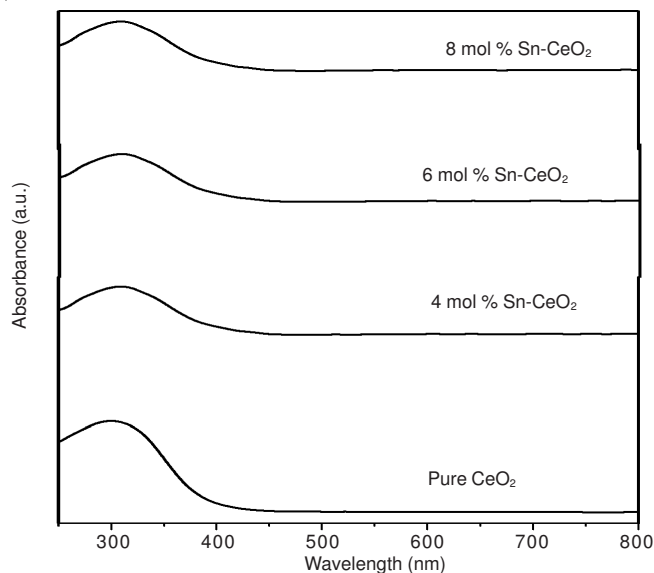


Fig. 5. (a) UV-visible absorption spectra of pure and Sn-doped CeO₂ nanoparticles

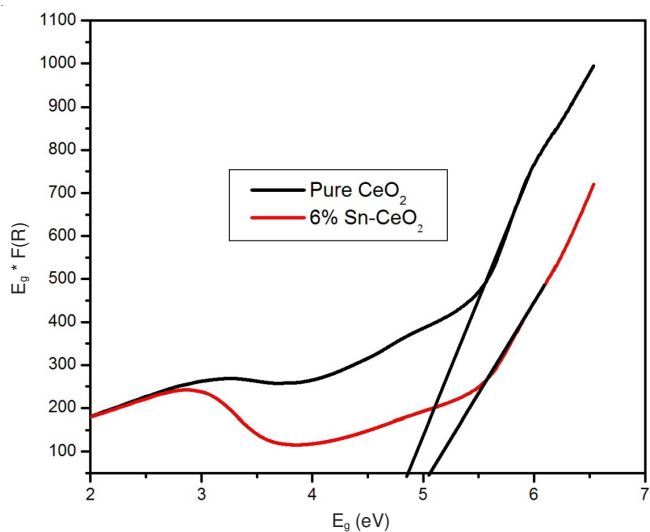


Fig. 5. (b) Energy band gap plots of pure and 6 mol % of Sn-doped CeO₂ nanoparticles

Conclusion

In summary, ultrafine Sn doped and undoped cerium oxide nanoparticles are successfully synthesized using simple chemical precipitation method. From the XRD analysis, it is found that the obtained nanopowders were in single phase cubic structure with an average particle size in the range 25-17 nm for the pure and doped samples. Moreover, the FT-IR study confirm the presence of pure and Sn doped CeO₂ nanoparticles. The SEM observation clearly reveals that the particles are strongly aggregated and appears in porous

morphology. UV-visible spectra states that absorption of both the pure and Sn-doped nanoparticles occurs at the UV region. The obtained optical band gap value ascribes to the most probable electron-hole confinement which leads to the high conductivity.

REFERENCES

1. G.R. Leandro, M.S.A. Jose and L.H. Miguel, *J. Nano Lett.*, **9**, 1395 (2009).
2. E.P. Murray, T. Tsai and S.A. Barnett, *Nature*, **400**, 649 (1999).
3. M. Hirano and E. Kato, *J. Am. Ceram. Soc.*, **82**, 786 (1999).
4. D. Bailey, L. Chow, S. Merchant and S.C. Kuiry, *J. Nat. Biotechnol.*, **14**, 112 (2003).
5. G.R. Bamwenda and H.J. Arakawar, *J. Mol. Catal. A*, **161**, 105 (2006).
6. A. Corma, P. Atienzer, H. Garcia and J.Y. Chang-Ching, *J. Nat. Mater.*, **3**, 394 (2004).
7. V.S. Vaishnav, P.D. Patel and N.G. Patel, *J. Mater. Manufact. Process.*, **21**, 257 (2006).
8. M.L. Dos Santos, R.C. Lima and C.S. Riccardi, *J. Mater. Lett.*, **62**, 4509 (2008).
9. J.J. Gulicovski, S.K. Milonjic and K.M. Szecsenyi, *J. Mater. Manufact. Process.*, **24**, 1080 (2009).
10. M.G. Sujana, K.K. Chattopadhyay and S. Anand, *J. Appl. Surf. Sci.*, **254**, 7405 (2008).
11. E. Finocchio, M. Daturi, C. Binet, J.C. Lavalley and G. Blanchard, *J. Catal. Today*, **52**, 53 (1999).
12. M. Zawadzki, *J. Alloys Comp.*, **454**, 347 (2008).
13. K. Chanjira and P. Sukon, *J. Microsc. Soc. Thailand*, **23**, 83 (2009).
14. K. Karthik, S.K. Pandian, K.S. Kumar and N.V. Jaya, *J. Appl. Surf. Sci.*, **256**, 4757 (2010).
15. S.K. Sahoo, M. Mohapatra, A.K. Singh and S. Anand, *J. Mater. Manufact. Process.*, **25**, 982 (2010).
16. S. Debnath, M.R. Islam and M.S.R. Khan, *J. Bull. Mater. Sci.*, **30**, 315 (2007).
17. H. Wang, J.-J. Zhu, J.-M. Zhu, X.-H. Liao, S. Xu, T. Ding and H.-Y. Chen, *J. Phys. Chem. Chem. Phys.*, **4**, 3794 (2002).